Electronic Supplementary Material (ESI) for New Journal of Chemistry.

Supporting Information

Structural transitions during Ni nanoparticle formation by decomposition of a Ni-containing metal-organic framework using *in-situ* total scattering

Nils Prinz[1], Sven Strübbe[2], Matthias Bauer[2], Mirijam Zobel[1,*]

[1] *Institute of Crystallography, RWTH Aachen University, 52066 Aachen, Germany*

[2] *Department of Chemistry and Center for Sustainable Systems Design, Paderborn University, 33098 Paderborn, Germany*

Contents

General Information

PDF refinement procedures

The refinements were done with *DiffPy-CMI*, a python-based complex modelling software.[1] During the least squares refinements, we refined the lattice parameters, the isotropic atomic thermal motion parameter B_{iso}, the correlated motion of nearest neighbors δ_2,[2] the spherical crystallite diameter (based on an isotropic attenuated crystal model) and a scale factor. The goodness of fit is described by the least square residuum R_w:

$$R_w = \sqrt{\frac{\sum_n (G_{obs,n} - G_{calc,n})^2}{\sum_n G_{obs,n}^2}}$$

Clausius-Clapeyron Equation

The Clausius-Clapeyron equation was used to determine the boiling pressure of DMF at 220 °C.[3]

$$\ln\left(\frac{p_2}{p_1}\right) = \frac{\Delta H_v}{R}\left(\frac{1}{T_1} - \frac{1}{T_2}\right)$$

p: pressure of the liquid at the boiling point

ΔH_v: Vaporization Enthalpy (46.9 kJ/mol)[4]

R: ideal gas constant

T: Boiling temperature

Temperature induced changes in Ni(BDC)(PNO) – supplementary PDF and PXRD

Table S 1: PDF refinement results of He-500.

R_w	T / °C	a / Å	b / Å	c / Å	Size / Å	B_{iso}(C) Å²	B_{iso}(O1) Å²	B_{iso}(O7) Å²	B_{iso}(Ni) Å²
0.39	20	19.155	7.113	9.283	42	4.0	0.9	2.2	0.5
0.39	25	19.153	7.115	9.286	42	4.0	1.0	2.2	0.5
0.40	30	19.154	7.115	9.288	42	4.0	0.9	2.2	0.5
0.40	35	19.156	7.115	9.291	42	4.0	0.8	2.2	0.5
0.39	40	19.153	7.114	9.297	42	4.0	0.9	2.3	0.5
0.40	45	19.157	7.110	9.300	43	3.1	0.9	2.0	0.5
0.39	50	19.149	7.118	9.299	42	4.0	1.2	2.2	0.5
0.39	55	19.145	7.120	9.299	42	4.0	1.1	2.1	0.5
0.39	60	19.149	7.113	9.309	44	3.6	1.0	1.9	0.6
0.39	65	19.137	7.118	9.309	42	3.4	1.0	2.1	0.5
0.40	70	19.149	7.119	9.311	44	4.0	1.0	2.1	0.6
0.39	75	19.145	7.121	9.312	43	4.0	1.0	2.1	0.6
0.40	80	19.136	7.122	9.315	42	3.4	1.0	2.1	0.5
0.40	85	19.139	7.119	9.319	44	3.5	1.0	2.2	0.6
0.39	90	19.133	7.127	9.319	43	4.0	1.1	2.2	0.6
0.47	95	19.139	7.122	9.328	42	4.0	0.5	2.1	0.6
0.43	100	19.148	7.115	9.332	43	3.5	1.1	2.1	0.6
0.43	105	19.136	7.131	9.322	43	3.9	1.6	2.0	0.6
0.40	110	19.134	7.129	9.329	43	4.0	1.3	2.1	0.6
0.48	115	19.133	7.129	9.337	43	4.0	0.7	1.9	0.6
0.40	120	19.136	7.130	9.337	43	4.0	1.3	2.1	0.6
0.48	125	19.138	7.132	9.342	43	4.0	0.9	1.9	0.6
0.48	130	19.135	7.132	9.346	43	4.0	1.0	1.9	0.6
0.40	135	19.131	7.133	9.345	43	4.0	1.4	2.1	0.7
0.44	140	19.122	7.127	9.360	43	3.2	1.2	2.0	0.6
0.48	145	19.139	7.131	9.358	43	4.0	0.9	2.0	0.7
0.41	150	19.133	7.135	9.354	43	4.0	1.4	2.2	0.7
0.48	155	19.133	7.134	9.364	43	4.0	0.8	2.0	0.7
0.49	160	19.128	7.138	9.364	42	4.0	1.0	1.9	0.7
0.49	165	19.129	7.135	9.371	42	4.0	1.0	2.0	0.7
0.49	170	19.129	7.136	9.375	43	4.0	1.0	2.1	0.7
0.49	175	19.135	7.133	9.380	43	4.0	0.8	2.1	0.7
0.48	180	19.132	7.138	9.377	42	4.0	1.2	2.0	0.7
0.49	185	19.131	7.137	9.381	42	4.0	1.2	1.9	0.7
0.49	190	19.131	7.138	9.385	42	4.0	1.1	2.0	0.7
0.49	195	19.130	7.138	9.386	42	4.0	1.2	2.0	0.7
0.48	200	19.131	7.141	9.385	41	4.0	1.3	1.9	0.8
0.49	205	19.131	7.138	9.393	43	4.0	1.3	2.0	0.8
0.49	210	19.132	7.139	9.389	41	4.0	1.2	2.0	0.8
0.49	215	19.136	7.141	9.388	41	4.0	1.3	2.0	0.8
0.50	220	19.132	7.138	9.389	41	4.0	1.3	2.0	0.8
0.50	225	19.129	7.137	9.387	40	4.0	1.2	1.9	0.8
0.52	230	19.128	7.138	9.385	41	4.0	1.2	2.0	0.8

0.52	235	19.133	7.134	9.389	40	4.0	1.1	2.1	0.9
0.53	240	19.125	7.129	9.393	38	4.0	0.9	2.2	0.9
0.54	245	19.119	7.128	9.400	38	4.0	0.9	2.3	0.9
0.54	250	19.109	7.128	9.399	36	4.0	1.0	2.1	1.0
0.55	255	19.114	7.124	9.402	36	4.0	0.9	2.4	1.0
0.56	260	19.109	7.127	9.402	35	4.0	0.9	2.1	1.1
0.57	265	19.106	7.125	9.403	35	4.0	0.8	2.1	1.2
0.58	270	19.097	7.126	9.406	34	4.0	0.8	2.2	1.2
0.59	275	19.103	7.121	9.407	34	4.0	0.7	2.2	1.2
0.60	280	19.087	7.120	9.410	34	4.0	0.7	2.2	1.3
0.61	285	19.076	7.123	9.412	33	4.0	0.7	2.2	1.3
0.61	290	19.071	7.118	9.413	33	4.0	0.7	2.2	1.4
0.62	295	19.083	7.110	9.427	37	4.0	0.2	2.1	1.7
0.63	300	19.065	7.119	9.417	31	4.0	0.6	2.3	1.5
0.63	305	19.066	7.110	9.421	32	4.0	0.5	2.3	1.5
0.64	310	19.080	7.097	9.412	30	4.0	0.4	2.3	1.5
0.65	315	19.194	7.045	9.366	26	4.0	0.1	2.5	1.5
0.66	320	19.280	6.998	9.337	25	4.0	0.1	2.5	1.5
0.70	325	19.491	6.834	9.281	24	1.7	0.2	2.5	1.0
0.69	330	19.443	6.905	9.291	23	4.0	0.1	2.5	1.4
0.73	335	19.621	6.724	9.214	22	1.1	0.3	2.5	0.8
0.76	340	19.758	6.699	9.188	21	0.9	0.4	2.5	0.8
0.81	345	20.255	6.653	9.180	21	0.5	0.6	2.5	1.2

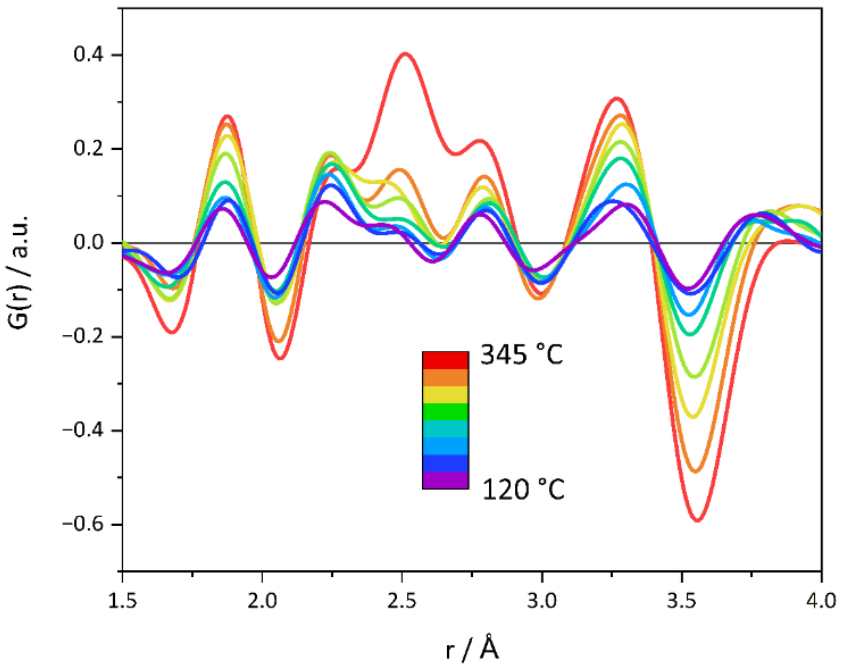

Figure S1: Difference-PDFs generated by the difference of the PDF(T_n)-PDF(20 °C) of He-500.

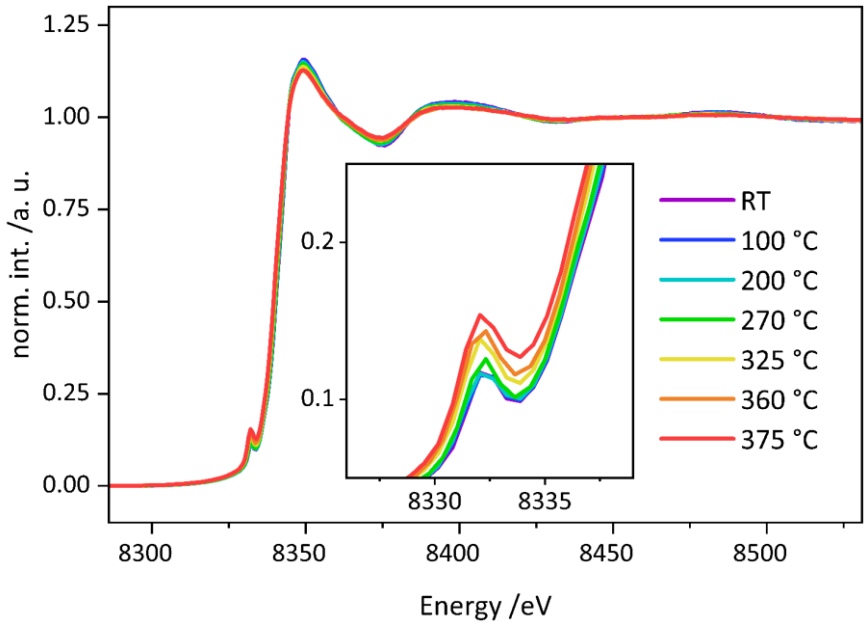

Figure S2: XANES spectra of He-375. The distortion of the framework is visible in the small change in the pre-peak region (inset).

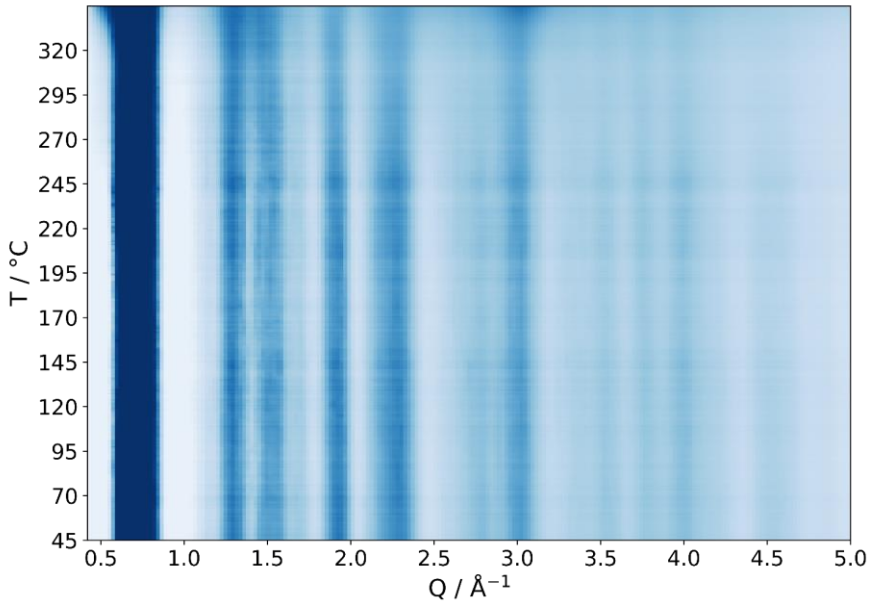

Figure S3: Heatmap of *in-situ* PXRD measurements of He–500 with rising temperature. The y-axis shows temperatures up to 345 °C.

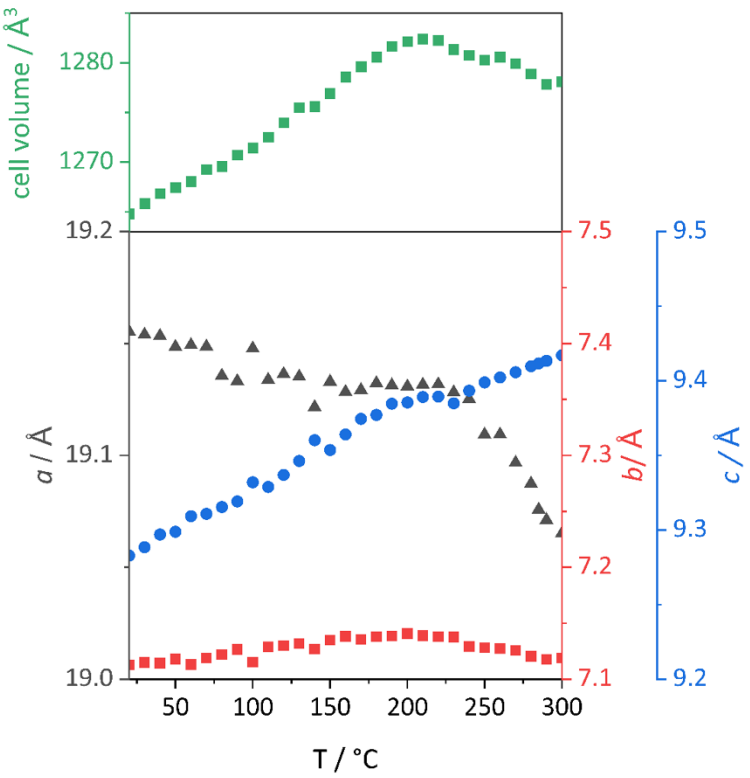

Figure S4: Lattice parameters *a* (black triangles), *b* (red squares) and *c* (blue dots), and resulting unit cell volume *V* (green squares) from PDF refinements of He–500.

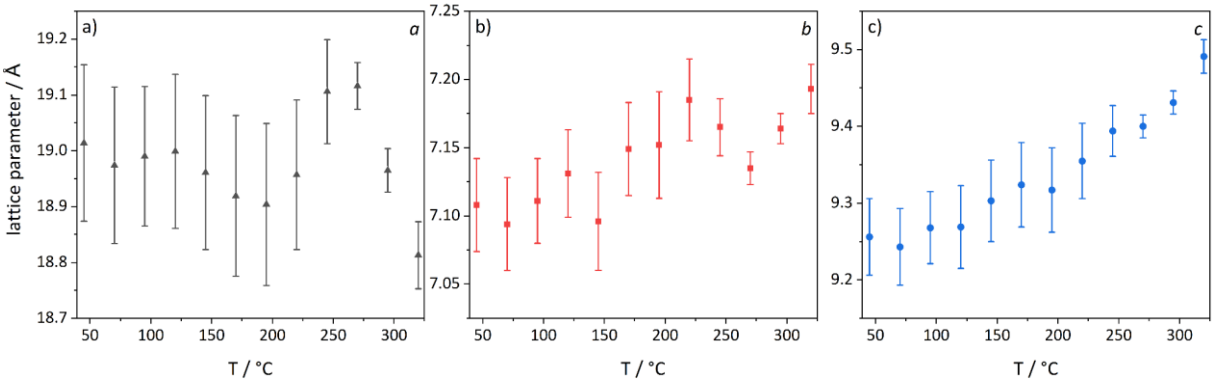

Figure S5: Rietveld refinements of He-500 with lattice parameter a) *a* (black triangles), b) *b* (red squares), c) *c* (blue dots).

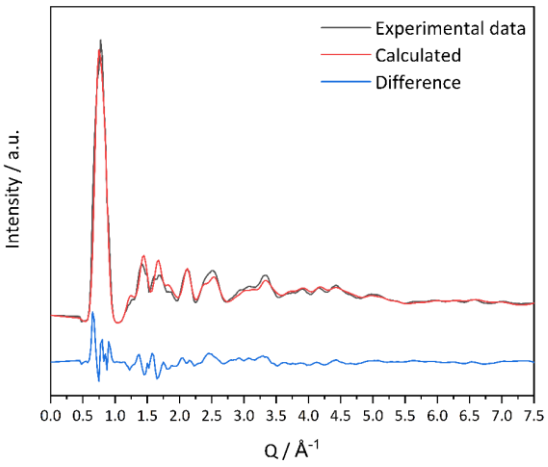

Figure S6: Rietveld refinement of He-500 at 200 °C.

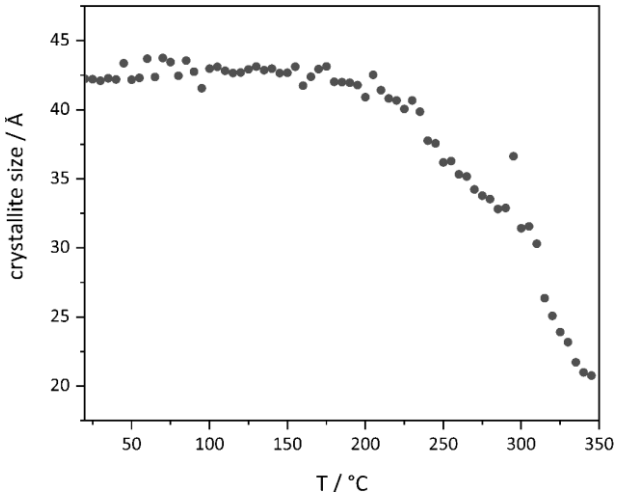

Figure S7: Amorphization of MOF framework during He-500 visible in the decreasing refined crystallite size for increasing temperature.

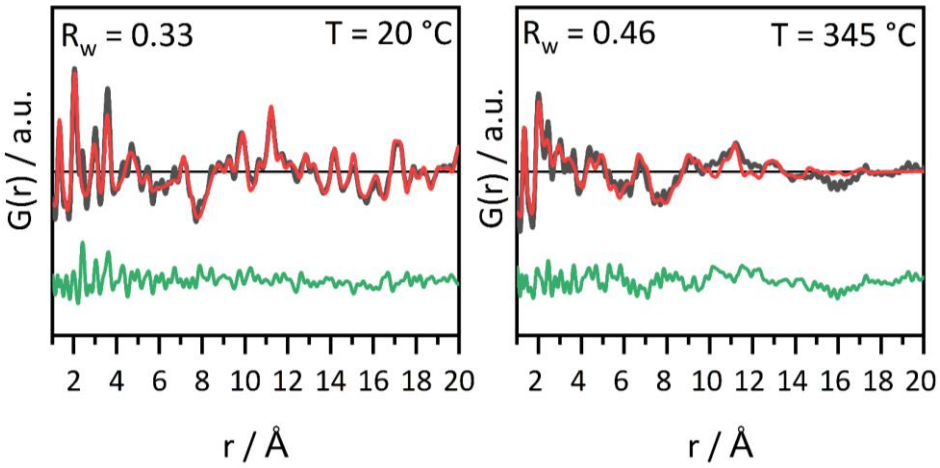

Figure S8: PDF refinements of Ni(BDC)(PNO) at 20 °C and 345 °C in He atmosphere. The goodness of fit is better at 20 °C, which can be explained by the overall higher crystallinity. At 345 °C the framework is in the process of collapsing and the long-range order is not visible anymore. Experimental data in black, fit in red, difference curve in green in offset.

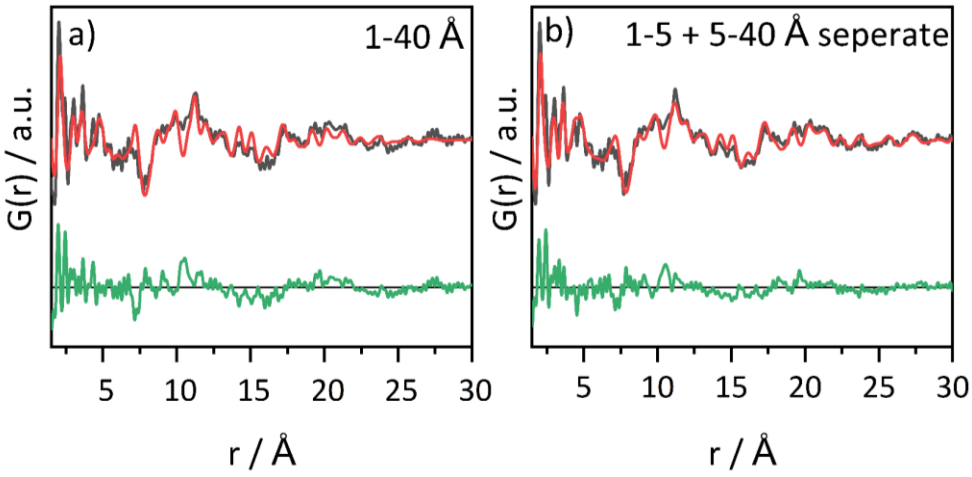

Figure S9: PDF refinement of Ni(BDC)(PNO) in He atmosphere at 245 °C. a) Fitted with one model in the range 1-40 Å. b) Combined refinement of the range 1-5 and 5-40 Å to account for the different B_{iso} of intra- (< 5 Å) and intermolecular (> 5 Å) carbon of the benzene-rings caused by the rotational freedom of the linker. Experimental data in black, fit in red, difference curve in green in offset.

NMF-mapping

Table S2: Temperatures and holding times where the MOF was 50% decomposed according to the NMF calculations.

Decomposition conditions	MOF 50 % decomposed
10% H_2 – 342 °C	56 min at 342 °C
10% H_2 – 375 °C	16 min at 375 °C
10% H_2 – 411 °C	During ramp at 396 °C
10% H_2 – 500 °C	During ramp at 393 °C
He – 500 °C	During ramp at 418 °C

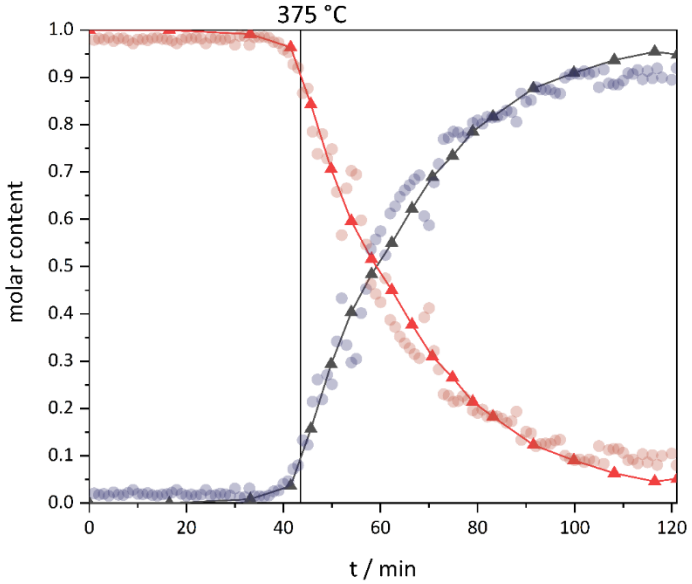

Figure S10: NMF weights as molar content from NMF mapping for the MOF (red line and triangles) and Ni (grey line and dots) compared with the molar contents found by PDF refinements (transparent dots, red and grey respectively for MOF and Ni).

Thermogravimetric Analysis coupled with mass spectroscopy (TGA-MS)

The total weight% of Ni in Ni(BDC)(PNO) can be calculated from the molar weight ratio:

$$\frac{M(Ni)}{M(Ni(BDC)(PNO)} = \frac{58.69\ g\ mol^{-1}}{317.91\ g\ mol^{-1}} = 0.185 = 18.5\ wt.\%$$

The experiments showed, that ca. 8 wt% solvent was still in the crystal. Therefore, the achievable relative mass of Ni would be 0.185*0.92=0.170 = 17 wt%. To calculate when 50% of the MOF is decomposed, we performed the calculation 0.92-((0.92-0.17)/2) = 0.545 = 54.5 relative weight%.

For comparison of the TGA data with the PDF refinements and the NMF mapping, the data of the TGA was normalized to 0 and 100%, where 0% is the point where the organic linker left the framework structure according to the MS analysis.

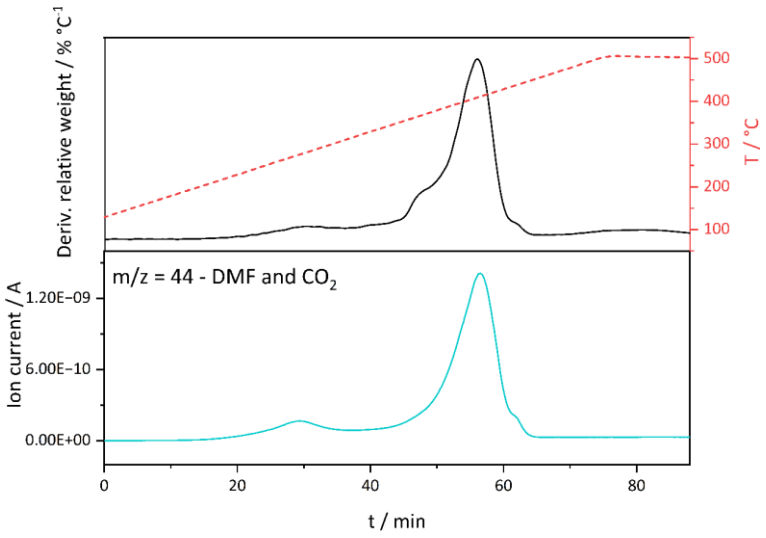

Figure S11: TGA-MS of $10H_2$-500. The m/z signal corresponding to DMF and CO_2 is shown.

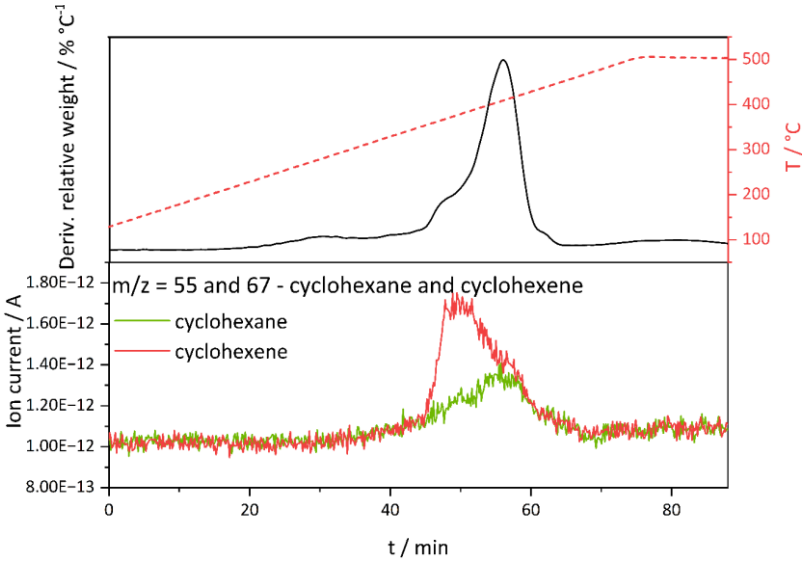

Figure S12: TGA-MS of $10H_2$-500. The m/z signal corresponding to cyclohexane and cyclohexene is shown.

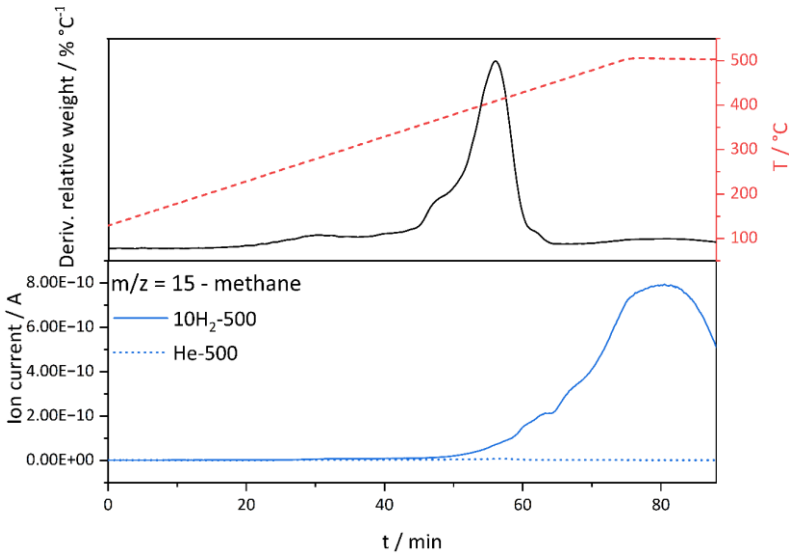

Figure S13: TGA-MS comparison between $10H_2$-500 and He-500. The m/z of 15 corresponds to CH_4. At higher temperatures CH4 is only formed in reductive atmosphere.

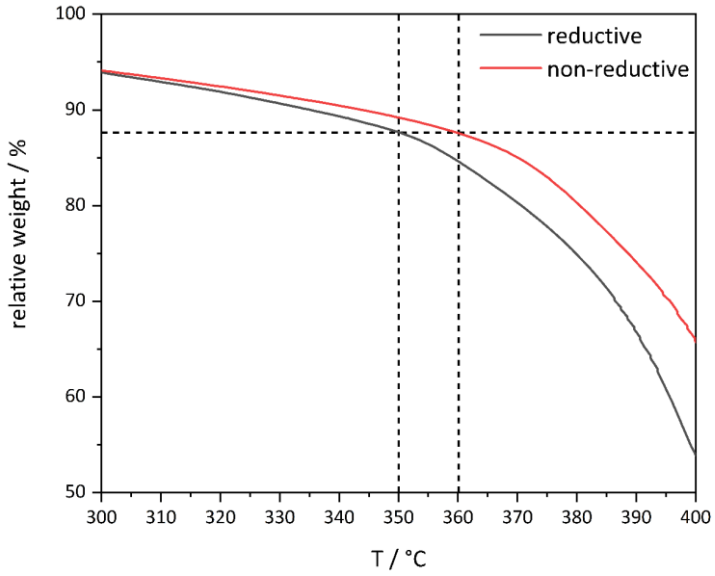

Figure S14: TGA of $10H_2$-500 and He-500. The same relative weight of 88% is achieved at 350 and 360 °C, respectively.

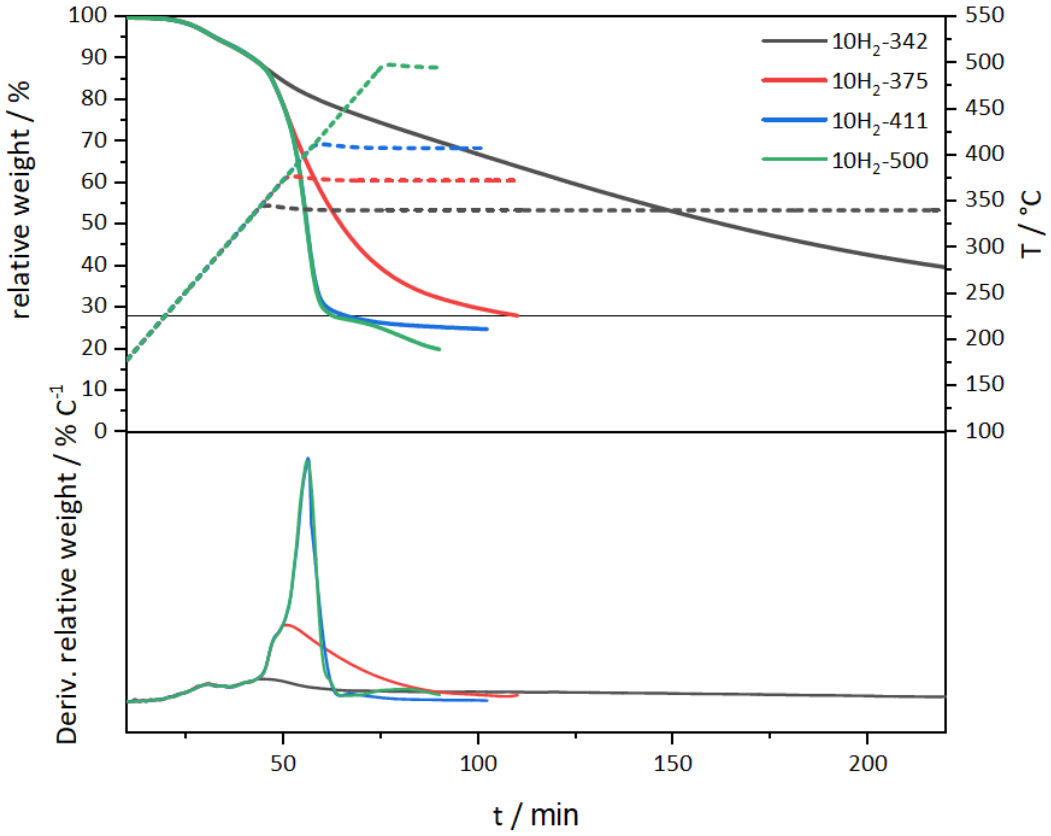

Figure S 15: TGA measurements with relative mass loss (top) and their derivatives (bottom). The corresponding temperature curves are shown with dashed lines.

X-ray data during formation of the catalyst in reductive atmosphere

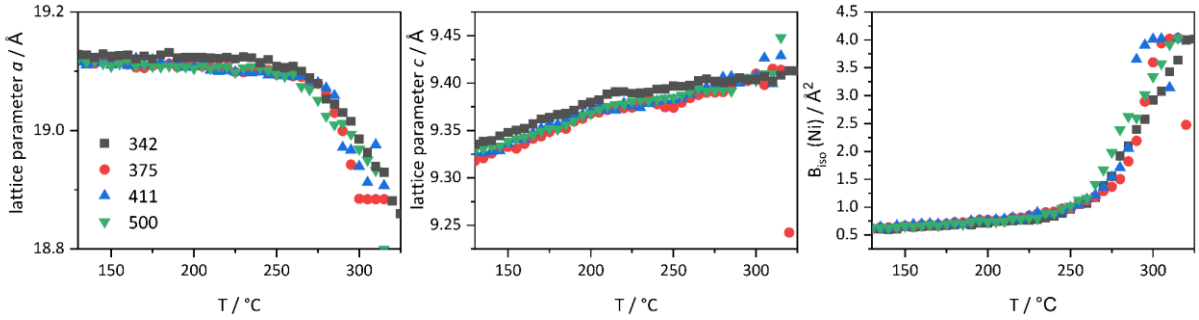

Figure S16: Lattice parameter *a* and *c* and thermal displacement parameter B_{iso}(Ni) of Ni(BDC)(PNO) from PDF refinements of 10H_2–342, 375, 411, 500. The low scattering of datapoints underpins the reproducibility of the experiments.

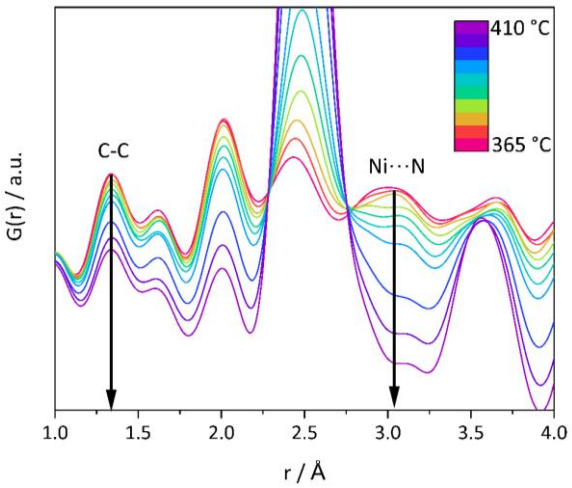

Figure S17: Experimental PDFs of $10H_2$-500 in the temperature range 365-410 °C. The distances C-C and Ni···N are highlighted.

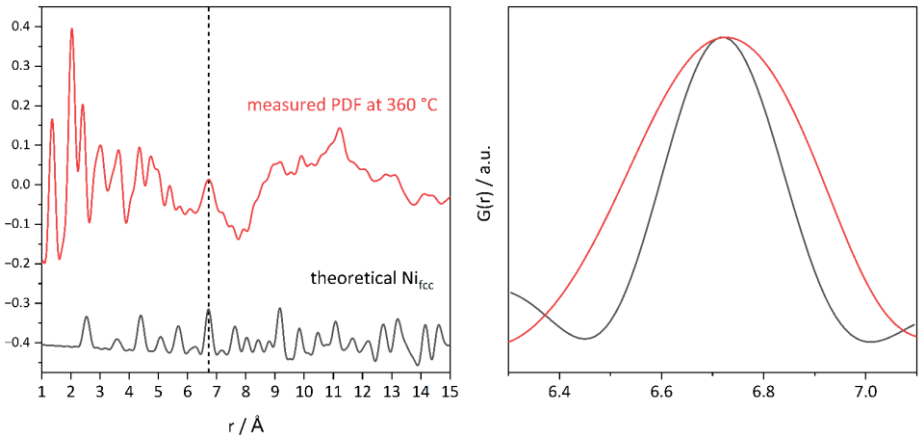

Figure S18: Comparison between the first observed clusters during $10H_2$-375 in the experimental PDF and a theoretical Ni_{fcc} structure (calculated with experimental instrumental resolution parameters). The measured PDF peaks appear much broader than the theoretical Ni structure predicts. In the right panel, the peak at 6.63 Å is enlarged for comparison.

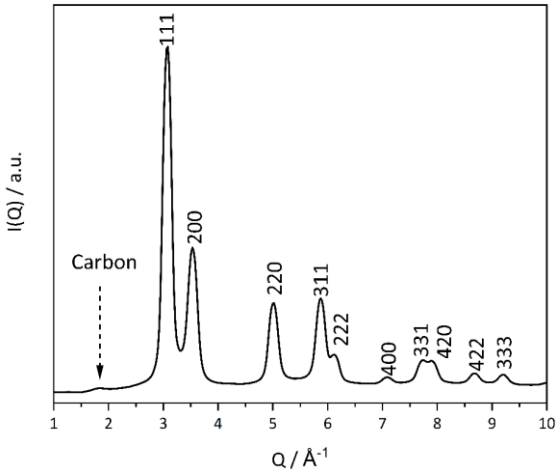

Figure S19: PXRD after holding time of 60 minutes of 10H2-375. A graphitic carbon residual is highlighted by the arrow.

Table S3: PDF refinement results of $10H_2$-375.

R_w	t / min	MOF *a* / Å	MOF *b* / Å	MOF *c* / Å	Ni *a* / Å	MOF size / Å	Ni size / Å	$B_{iso}(Ni_{fcc})$ Å²	MOF molar fraction	Ni molar fraction
0.36	1	19.116	7.147	9.316	-	42	-	-	>0.90	<0.10
0.36	2	19.112	7.145	9.321	-	42	-	-	>0.90	<0.10
0.37	3	19.112	7.151	9.318	-	42	-	-	>0.90	<0.10
0.38	4	19.110	7.141	9.329	-	42	-	-	>0.90	<0.10
0.36	5	19.118	7.152	9.326	-	42	-	-	>0.90	<0.10
0.37	6	19.112	7.155	9.328	-	42	-	-	>0.90	<0.10
0.37	7	19.112	7.156	9.326	-	42	-	-	>0.90	<0.10
0.36	8	19.110	7.161	9.329	-	42	-	-	>0.90	<0.10
0.35	9	19.121	7.165	9.331	-	42	-	-	>0.90	<0.10
0.37	10	19.101	7.160	9.337	-	42	-	-	>0.90	<0.10
0.37	11	19.103	7.157	9.343	-	42	-	-	>0.90	<0.10
0.36	12	19.113	7.167	9.343	-	42	-	-	>0.90	<0.10
0.38	13	19.104	7.153	9.348	-	42	-	-	>0.90	<0.10
0.37	14	19.110	7.166	9.349	-	42	-	-	>0.90	<0.10
0.36	15	19.120	7.169	9.351	-	42	-	-	>0.90	<0.10
0.36	16	19.115	7.169	9.356	-	42	-	-	>0.90	<0.10
0.36	17	19.114	7.169	9.358	-	42	-	-	>0.90	<0.10
0.34	18	19.123	7.168	9.359	-	42	-	-	>0.90	<0.10
0.35	19	19.110	7.171	9.363	-	42	-	-	>0.90	<0.10
0.36	20	19.111	7.173	9.362	-	42	-	-	>0.90	<0.10
0.36	21	19.099	7.175	9.361	-	42	-	-	>0.90	<0.10
0.37	22	19.106	7.177	9.365	-	42	-	-	>0.90	<0.10
0.37	23	19.094	7.173	9.365	-	42	-	-	>0.90	<0.10
0.36	24	19.106	7.173	9.360	-	41	-	-	>0.90	<0.10
0.37	25	19.097	7.171	9.357	-	41	-	-	>0.90	<0.10
0.37	26	19.080	7.176	9.358	-	41	-	-	>0.90	<0.10
0.38	27	19.074	7.178	9.361	-	41	-	-	>0.90	<0.10
0.38	28	19.073	7.172	9.364	-	41	-	-	>0.90	<0.10
0.42	29	19.053	7.152	9.379	-	41	-	-	>0.90	<0.10
0.37	30	19.050	7.186	9.362	-	40	-	-	>0.90	<0.10
0.42	31	19.052	7.147	9.383	-	38	-	-	>0.90	<0.10
0.43	32	19.038	7.149	9.383	-	40	-	-	>0.90	<0.10
0.38	33	19.021	7.204	9.350	-	38	-	-	>0.90	<0.10
0.46	34	19.014	7.119	9.397	-	37	-	-	>0.90	<0.10
0.45	35	18.991	7.139	9.388	-	36	-	-	>0.90	<0.10
0.46	36	18.972	7.125	9.394	-	36	-	-	>0.90	<0.10
0.47	37	18.988	7.101	9.380	-	33	-	-	>0.90	<0.10
0.50	38	19.151	6.966	9.312	-	29	-	-	>0.90	<0.10
0.50	39	19.145	6.947	9.309	-	28	-	-	>0.90	<0.10
0.53	40	19.183	6.784	9.293	-	27	-	-	>0.90	<0.10
0.52	41	19.200	6.784	9.275	-	28	-	-	>0.90	<0.10
0.55	42	19.271	6.784	9.256	-	25	-	-	>0.90	<0.10
0.49	43	19.170	6.784	9.249	-	28	-	-	>0.90	<0.10

0.61	44	19.297	6.784	9.242	3.576	23	20	1.0	0.87	0.13
0.32	45	19.153	6.784	9.469	3.565	39	29	1.4	0.88	0.12
0.50	46	19.280	6.784	9.253	3.569	20	24	1.0	0.79	0.21
0.44	47	19.312	6.784	9.257	3.565	20	24	1.0	0.74	0.26
0.26	48	19.256	6.784	9.308	3.559	25	32	1.4	0.78	0.22
0.21	49	19.242	6.784	9.327	3.559	38	32	1.3	0.73	0.27
0.22	50	19.473	6.784	9.264	3.558	20	33	1.4	0.75	0.25
0.24	51	19.443	6.784	9.188	3.558	20	31	1.3	0.66	0.34
0.28	52	19.359	6.784	9.269	3.557	20	30	1.0	0.57	0.43
0.18	53	19.684	6.784	9.167	3.556	22	34	1.3	0.67	0.33
0.16	54	19.684	6.784	8.959	3.555	22	35	1.2	0.70	0.30
0.15	55	19.684	6.784	8.918	3.555	21	35	1.2	0.69	0.31
0.15	56	19.684	6.784	9.195	3.554	27	35	1.2	0.60	0.40
0.17	57	18.975	7.251	8.884	3.554	20	34	1.2	0.55	0.45
0.17	58	18.884	7.528	9.259	3.553	36	35	1.2	0.46	0.54
0.16	59	18.884	7.523	9.249	3.553	37	35	1.2	0.44	0.56
0.16	60	18.884	7.548	9.241	3.553	37	35	1.2	0.42	0.58
0.14	61	18.884	7.311	9.077	3.553	32	35	1.2	0.48	0.52
0.15	62	18.884	7.557	9.243	3.552	38	36	1.2	0.39	0.61
0.14	63	18.884	7.570	9.234	3.552	38	36	1.2	0.37	0.63
0.14	64	18.884	7.574	9.235	3.551	39	36	1.2	0.35	0.65
0.14	65	18.884	7.568	9.239	3.551	39	36	1.2	0.34	0.66
0.13	66	18.884	7.576	9.239	3.551	39	36	1.1	0.33	0.67
0.13	67	18.884	7.580	9.228	3.551	38	36	1.1	0.32	0.68
0.13	68	18.884	7.583	9.224	3.550	39	36	1.1	0.31	0.69
0.12	69	18.933	7.414	8.884	3.551	20	36	1.1	0.39	0.61
0.12	70	18.953	7.419	8.884	3.551	20	36	1.1	0.41	0.59
0.12	71	18.892	7.433	8.884	3.550	20	35	1.1	0.32	0.68
0.12	72	18.884	7.584	9.176	3.549	38	36	1.1	0.28	0.72
0.12	73	18.884	7.584	9.222	3.549	39	36	1.1	0.23	0.77
0.11	74	18.884	7.584	9.190	3.549	39	36	1.1	0.23	0.77
0.11	75	18.884	7.584	9.213	3.549	36	36	1.1	0.21	0.79
0.11	76	18.884	7.584	9.208	3.549	35	36	1.1	0.22	0.78
0.11	77	18.885	7.584	9.234	3.549	33	36	1.1	0.23	0.77
0.11	78	18.884	7.584	9.186	3.549	37	36	1.1	0.22	0.78
0.11	79	18.884	7.584	9.213	3.549	33	36	1.1	0.20	0.80
0.11	80	18.884	7.584	9.214	3.548	33	36	1.1	0.19	0.81
0.11	81	18.884	7.584	9.180	3.548	44	36	1.1	0.20	0.80
0.11	82	18.884	7.584	9.198	3.548	37	36	1.1	0.18	0.82
0.10	83	18.884	7.584	9.180	3.548	45	36	1.1	0.19	0.81
0.10	84	18.884	7.584	9.197	3.548	39	36	1.1	0.18	0.82
0.10	85	18.884	7.584	9.169	3.547	32	36	1.1	0.18	0.82
0.10	86	18.885	7.584	9.169	3.548	28	36	1.1	0.17	0.83
0.10	87	18.884	7.584	9.146	3.548	28	36	1.1	0.17	0.83
0.10	88	18.884	7.580	9.172	3.547	27	36	1.1	0.19	0.81
0.10	89	18.884	7.584	9.181	3.549	53	36	1.1	0.13	0.87
0.10	90	18.884	7.584	9.190	3.550	43	36	1.1	0.15	0.85

0.10	91	18.884	7.584	9.182	3.550	46	36	1.1	0.15	0.85
0.10	92	18.884	7.584	9.178	3.550	53	36	1.1	0.12	0.88
0.10	93	18.884	7.584	9.167	3.550	51	36	1.1	0.13	0.87
0.10	94	18.884	7.584	9.164	3.549	50	36	1.1	0.13	0.87
0.10	95	18.884	7.584	9.163	3.548	44	36	1.1	0.13	0.87
0.10	96	18.884	7.584	9.159	3.548	48	36	1.1	0.13	0.87
0.10	97	18.884	7.584	9.159	3.548	48	36	1.1	0.13	0.87
0.10	98	-	-	-	3.548	-	36	1.1	<0.10	>0.90
0.10	99	-	-	-	3.547	-	36	1.1	<0.10	>0.90
0.10	100	-	-	-	3.547	-	35	1.1	<0.10	>0.90
0.10	101	-	-	-	3.547	-	35	1.1	<0.10	>0.90
0.10	102	-	-	-	3.547	-	35	1.1	<0.10	>0.90
0.10	103	-	-	-	3.547	-	35	1.1	<0.10	>0.90
0.10	104	-	-	-	3.546	-	35	1.1	<0.10	>0.90
0.09	105	-	-	-	3.546	-	35	1.1	<0.10	>0.90
0.09	106	-	-	-	3.546	-	35	1.1	<0.10	>0.90
0.10	107	-	-	-	3.546	-	35	1.1	<0.10	>0.90
0.09	108	-	-	-	3.546	-	35	1.1	<0.10	>0.90
0.09	109	-	-	-	3.546	-	35	1.1	<0.10	>0.90
0.09	110	-	-	-	3.546	-	35	1.1	<0.10	>0.90
0.09	111	-	-	-	3.546	-	35	1.1	<0.10	>0.90
0.09	112	-	-	-	3.546	-	35	1.1	<0.10	>0.90
0.09	113	-	-	-	3.545	-	35	1.0	<0.10	>0.90
0.09	114	-	-	-	3.545	-	35	1.0	<0.10	>0.90
0.09	115	-	-	-	3.545	-	35	1.0	<0.10	>0.90
0.09	116	-	-	-	3.545	-	35	1.0	<0.10	>0.90
0.09	117	-	-	-	3.545	-	35	1.0	<0.10	>0.90
0.09	118	-	-	-	3.545	-	35	1.0	<0.10	>0.90
0.09	119	-	-	-	3.546	-	35	1.0	<0.10	>0.90
0.09	120	-	-	-	3.545	-	35	1.0	<0.10	>0.90
0.09	121	-	-	-	3.546	-	35	1.0	<0.10	>0.90
0.09	122	-	-	-	3.546	-	35	1.0	<0.10	>0.90

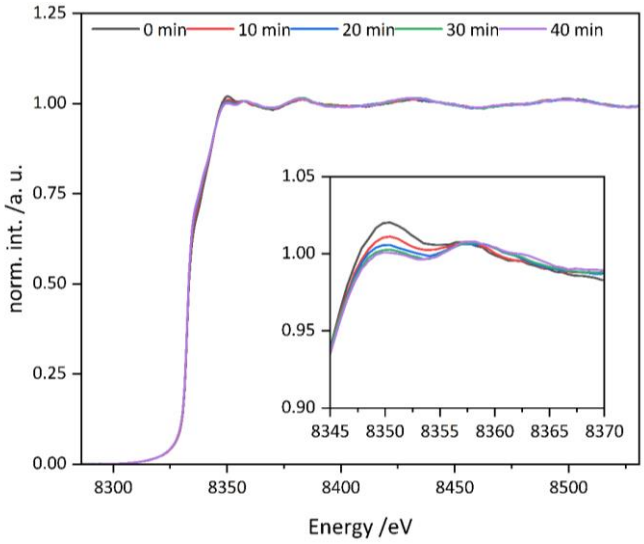

Figure S20: XANES spectra of 10H_2-500 after reaching the final temperature 500 °C. Inset is the zoom into the white line region, where the maxima of the first and second peak change their intensity ratio.

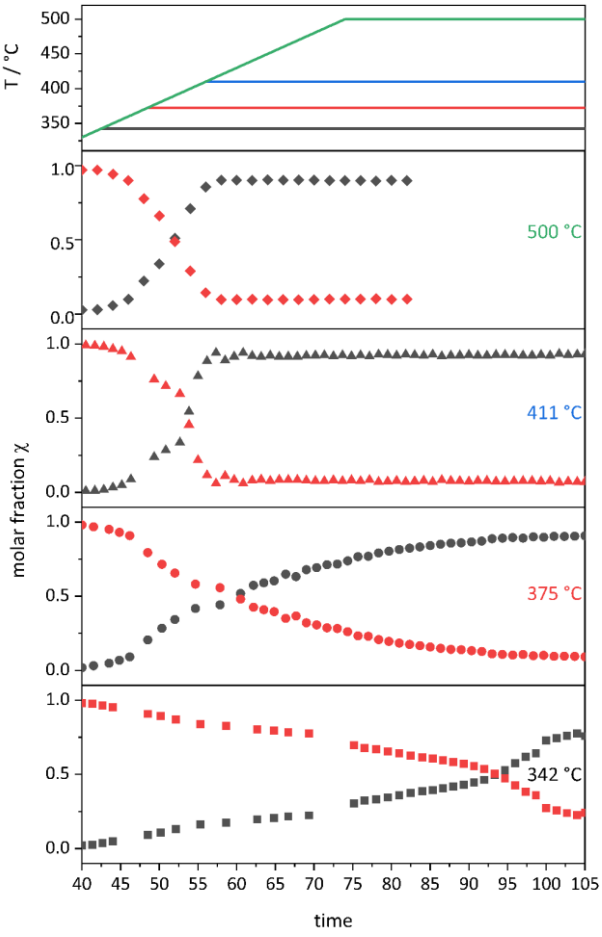

Figure S21: Molar fractions of Ni(BDC)(PNO) and Ni_{fcc} from PDF refinements during the course of decomposition.

X-ray scattering data during formation of the catalyst in non-reductive atmosphere

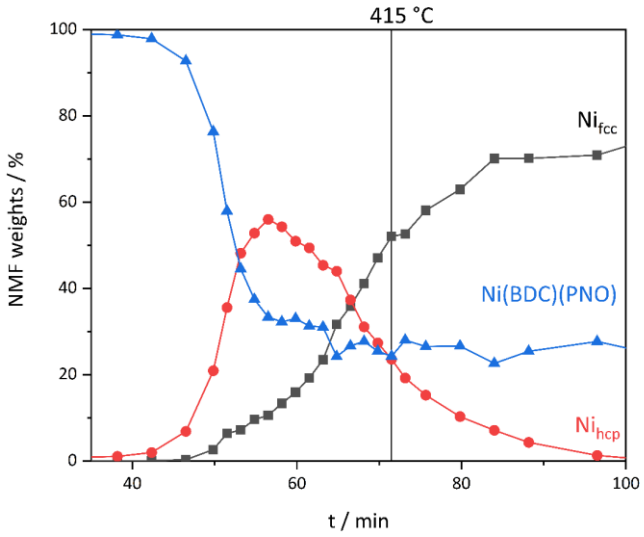

Figure S22: Results of NMF mapping of the decomposition under He and 500 °C end temperature. Three components were needed for a reliable NMF mapping. Note, that the Ni(BDC)(PNO) weight is not approaching zero.

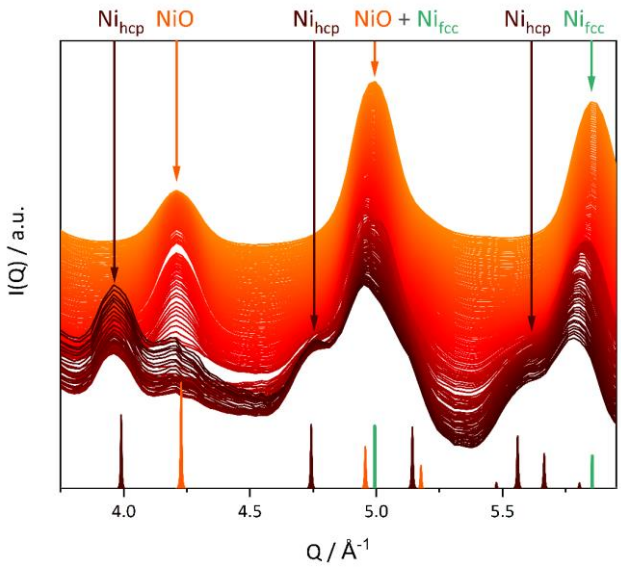

Figure S23: *In-situ* PXRDs of Ni(BDC)(PNO) decomposed in He with final temperature of 500 °C in the timeframe 50 – 71 min during heat ramp of 5 °C/min starting at 405 °C at 70 min.

References

1 P. Juhás, C. L. Farrow, X. Yang, K. R. Knox and S. J. L. Billinge, Complex modeling: a strategy and software program for combining multiple information sources to solve ill posed structure and nanostructure inverse problems, *Acta Crystallogr., Sect. A: Found. Adv.*, 2015, **71**, 562–568. DOI: 10.1107/S2053273315014473.

2 I.-K. Jeong, R. H. Heffner, M. J. Graf and S. J. L. Billinge, Lattice dynamics and correlated atomic motion from the atomic pair distribution function, *Phys. Rev. B*, 2003, **67**. DOI: 10.1103/PhysRevB.67.104301.

3 U. Krey, *Basic theoretical physics. A concise overview*, Springer.

4 G. Barone, G. Castronuovo, G. Della Gatta, V. Elia and A. Iannone, Enthalpies of vaporization of seven alkylamides, *Fluid Phase Equilibria*, 1985, **21**, 157–164. DOI: 10.1016/0378-3812(85)90066-4.